

# Fully and double differential cross sections for the single ionization of H<sub>2</sub>O by bare ion impact.

L. Fernández-Menchero<sup>1,2</sup> and S. Otranto<sup>3</sup>

<sup>1</sup>Atomic Data and Analysis Structure, Department of Physics, University of Strathclyde, United Kingdom

<sup>2</sup>Max-Planck-Institut für Plasmaphysik, Boltzmannstraße 2, D-85748 Garching, Germany

<sup>3</sup>IFISUR and Departamento de Física, Universidad Nacional del Sur, Av. Alem 1253, 8000 Bahía Blanca, Argentina

**Abstract.** A theoretical study of fully differential cross sections for the single ionization of H<sub>2</sub>O by collisions with H<sup>+</sup>,  $\bar{p}^-$  and He<sup>2+</sup> at an impact energy of 2 and 6 MeV/amu is presented. We work in terms of the Born-3DW model, which considers in the final state a model central potential to represent the interaction of the emitted electron with the molecular core. Results are presented for the lesser bound molecular orbitals (1B<sub>1</sub>, 1B<sub>2</sub>, 2A<sub>1</sub> and 3A<sub>1</sub>). Doubly differential cross sections in terms of the electron emission angle are also presented for these molecular orbitals, showing a nearly isotropic distribution for the electron energies under consideration.

PACS numbers: 34.10.+x, 34.50.Fa, 52.20.Hv

Submitted to: *J. Phys. B: At. Mol. Phys.*

## 1. Introduction

Ionization of atoms and molecules by fast charged particles has been a matter of active research in the last two decades [1]. This could be partially due to the natural desire of increasing our understanding of the physics underlying in simple collision systems. It should be noted that at the fully differential level, collision processes involving the simplest possible targets (H and He) remained elusive at low impact energies until the last decade when numerically intensive methods provided what could be defined as definite cross sections for (e,2e) processes (see [2, 3, 4] and references therein). Besides, atomic processes are also relevant in many areas, like atmosphere physics, (fusion) plasma and astrophysics, for which there is a need of cross sections concerning charge exchange and ionization processes originated by charged particle impact. Those cross sections can be ulteriorly used to feed statistical models which track the energy deposition of a particle as it enters into the target area of interest. In this sense, ionization cross sections for ion impact on biological molecules could be useful in biology and medicine, in areas like radiobiology, medical imaging and radiotherapy as well [5]. It is worth noting that ion therapy has raised in recent years as a potential technique for treating cancer tumors and several facilities are currently under way like those at Heidelberg, Pavia, Marburg and Kiel.

From the experimental point of view, and starting in the mid-1990s, the development of the cold target recoil ion momentum spectroscopy (COLTRIMS) [6, 7, 8] technique, has provided a new insight on collision systems since it allowed to perform kinematically complete experiments of collision processes involving photons, ions, and electrons [9, 10, 11, 12]. Following the Frankfurt and Heidelberg groups, this technique has since then been adopted by several laboratories worldwide. Despite the limitations in the experimental setup (only low-energy emitted electrons are detected to avoid prohibitive extraction fields), a vast amount of data has been obtained for a large variety of collision systems. More recent works have been realized in ion-atom [13, 14, 15, 16], ion-molecule [17, 18, 19, 20, 21], and ion-cluster [22] collisions.

Theoretically, Fully Differential Cross Sections (FDCS) in ion-atom collisions have been calculated by means of continuum distorted waves models [23, 24, 25, 26, 27, 28, 29, 30, 31], by the classical trajectory Monte Carlo method (CTMC) [32, 33, 34, 35, 36], or applying other approximated methods [37, 38, 39, 40] for which this work could be a good testing reference. FDCS in ion-molecule collisions have been studied in terms of a Born-3DW model, assuming that the molecular potential is either purely Coulombic [41, 42], or a central potential which takes into account the multielectronic character of the resulting molecular ion [43, 44].

In a previous work [43], we presented the Born-3DW method to obtain the FDCS for single ionization of the CH<sub>4</sub> molecule by bare ion impact for impact energies in the order of MeV/amu. In this work, we consider the single ionization of the water molecule by fully stripped ions at high impact energies. We also integrate the FDCS in the projectile deflection angles and calculate the Double Differential Cross Sections

(DDCS) as a function of the electron emission angle. This target is of particular interest in astrophysics (largely populates cometary comas and planetary atmospheres), in radiobiology (where the water molecule resembles organic matter), or in fusion plasmas (where oxygen atoms are used for diagnosis and can react with the hydrogen forming at most water, and other species, like H<sub>3</sub>O<sup>+</sup>, OH<sup>-</sup> or H<sub>2</sub>O<sub>2</sub> in the cold zones of the plasma, like the divertors).

The paper is organized as follows: the next section is devoted to a brief description of the theoretical model in use. In section 3 we analyze the FDCS calculated in this work for the single ionization of water by H<sup>+</sup>,  $\bar{p}^-$  and He<sup>2+</sup> impact and the DDCS for the impact with alpha particle. In section 4 we draw our conclusions and outlook. Atomic units are used throughout this work unless otherwise stated.

## 2. Theoretical model

We consider a stripped ion of charge  $Z_P$  and mass  $M_P$  incident upon a multielectron molecular target of mass  $M_T$  in the ground state. We consider one active electron placed in the molecular orbital  $i$  of the ground state, so the initial wave function for the target can be written as  $\phi_i(\mathbf{r})$ . This wave function is an eigenfunction of the Schrödinger equation with a molecular model potential  $V_{\text{moli}}(\mathbf{r})$ , that includes the nuclei and the other electron terms:

$$V_{\text{moli}}(\mathbf{r}) = -\sum_{l=1}^M \frac{Z_l}{|\mathbf{r} - \mathbf{R}_l|} + \sum_{j=1}^{N_{MO}} N_{ij} \int d^3\mathbf{r}' \frac{|\phi_j(\mathbf{r}')|^2}{|\mathbf{r} - \mathbf{r}'|}, \quad (1)$$

where  $M$  is the number of nuclei which form the molecule,  $Z_l$  the charge each nuclei,  $\mathbf{R}_l$  their position respect the molecular center of mass,  $N_{MO}$  the number of molecular orbitals of the molecule and  $N_{ij}$  values 2 if  $i \neq j$ , and 1 if  $i = j$ , and  $\phi_j(\mathbf{r}')$  their one-electron wave functions. Following the steps of [43], we use the SCF-MO analytical expansions in terms of Slater functions provided by Moccia [45] for the five occupied orbitals of H<sub>2</sub>O in its ground state: 1A<sub>1</sub>, 2A<sub>1</sub>, 3A<sub>1</sub>, 1B<sub>2</sub> and 1B<sub>1</sub>. As the inner orbital 1A<sub>1</sub> is tightly bound ( $-20.5249$  a.u.), we neglect its contribution to the the ionization channel. The binding energies employed throughout this work are  $-1.3261$ ,  $-0.5561$ ,  $-0.6814$  and  $-0.4954$  a.u. for the 2A<sub>1</sub>, 3A<sub>1</sub>, 1B<sub>2</sub> and 1B<sub>1</sub> molecular orbitals respectively.

In the list of Moccia coefficients, we obtain the pairs  $(l, m)$  that contribute to the cross section for each molecular orbital and the parameters for these radial expansions in Slater functions  $a, n, \xi$  as follows:

$$\phi_i(\mathbf{r}) = \sum_{lm} \sum_{j=1}^k a_{lmij} \mathcal{R}_{n_{ij}\xi_{ij}}(r) Y_{lm}(\hat{\mathbf{r}}), \quad (2)$$

where  $\mathcal{R}_{n_{ij}\xi_{ij}}(r)$  are the Slater functions given by

$$\mathcal{R}_{n\xi}(r) = \sqrt{\frac{(2\xi)^{2n+1}}{(2n)!}} e^{-\xi r} r^{n-1}. \quad (3)$$

The expansion coefficients are shown in tables 1, 2, 3 and 4. This expansion correspond to a basis set of complex spherical harmonics  $Y_{lm}$  and not real ones  $C_{lm}$ ,  $S_{lm}$  as it is shown directly in [45]. Hence, the coefficients for  $m \neq 0$  differ in a factor  $\sqrt{2}$  and  $i$  imaginary unit.

The transition amplitude for single ionization can be written as

$$T_{fi} = \langle \Psi_f | V_I | \Psi_i \rangle, \quad (4)$$

where the initial channel wave function  $\Psi_i(\mathbf{K}_i; \mathbf{R}_i, \mathbf{r})$  is given by the wave function for the molecular orbital under consideration times an incident plane-wave for the incoming projectile:

$$\Psi_i = \frac{1}{(2\pi)^{3/2}} e^{i\mathbf{K}_i \cdot \mathbf{R}_i} \phi_i(\mathbf{r}). \quad (5)$$

Here,  $\mathbf{R}_i$  is the relative coordinate between the projectile and the center of mass of the target molecule before the collision. The final channel wave function  $\Psi_f(\mathbf{K}_f; \mathbf{R}_f, \mathbf{r})$  is written as

$$\begin{aligned} \Psi_f = & \frac{1}{(2\pi)^{3/2}} e^{i\mathbf{K}_f \cdot \mathbf{R}_f} C^-(\mathbf{K}_f; \mathbf{R}_f) \\ & \times \chi^-(\mathbf{k}; \mathbf{r}) C^-(\mathbf{k}_{eP}; \mathbf{R}_f - \mathbf{r}), \end{aligned} \quad (6)$$

where  $\mathbf{r}$  is the coordinate of the ejected electron with respect to the center of mass of the ionized target system,  $\mathbf{R}_f$  the position of the projectile with respect to the same origin after the collision;  $\chi^-(\mathbf{k}; \mathbf{r})$  represents a final continuum wave function ( $E > 0$ ) for the emitted electron with a determined momentum  $\mathbf{k}$  subject to the potential  $V_{\text{moli}}(\mathbf{r})$ ,  $C^-(\mathbf{K}_f, \mathbf{R}_f)$ ,  $C^-(\mathbf{k}_{eP}, \mathbf{R}_f - \mathbf{r})$  are the Coulombian distortions for the internuclear interaction and the emitted electron-projectile subsystem respectively. The interaction potential  $V_I$  is given by the non-resolved part of the Hamiltonian by the initial state:

$$V_I(\mathbf{R}_i, \mathbf{r}) = -\frac{Z_P}{|\mathbf{r} - \mathbf{R}_i|} - Z_P V_{\text{moli}}(\mathbf{R}_i). \quad (7)$$

We do not use the real anisotropic potential  $V_{\text{moli}}(\mathbf{r})$  shown in (1) but a radial  $U_i(r)$  resulting of its angular integration instead:

$$U_i(r) = \frac{1}{4\pi} \int_{4\pi} d\Omega V_{\text{moli}}(\mathbf{r}). \quad (8)$$

As a result, the emitted electron sees the nuclear charge of the central atom (that for the water molecule would be +8) in the limit  $r \rightarrow 0$ , and the asymptotic charge  $Z_{\text{asint}} = +1$  as  $r \rightarrow \infty$ . The introduction of this form for the potential seen by the emitted electron, strongly influences the way in which the electron is attracted by the parent molecular ion while in the reaction region compared to the asymptotic form  $Z_{\text{asint}}/r$ . Such a description is considered to be much more appropriate and is expected to play a clear role in the angular distributions by affecting the shape and intensity of the denominated ‘‘recoil peak’’. This structure, represents second order collisions between the emitted electron and the molecular parent ion and gains importance as the emitted

electron momentum  $k_e$  is greater than the momentum transferred by the projectile ( $q$ ). In addition, we recall that future experiments with oriented molecules will probably face theoreticians with the need of developing a full anisotropic treatment for the emitted electron-molecular ion potential.

The FDCS for a particular orientation of the water molecule is then a function of the three Euler angles  $(\alpha, \beta, \gamma)$ ,

$$\frac{d^8\sigma}{d^2\mathbf{q}_\perp d^3\mathbf{k} d\alpha d\beta d\gamma} = (2\pi)^4 N_e \frac{\mu_{Ie}\mu_{PT}^2}{K_i K_f} |T_{fi}(\mathbf{q}, \mathbf{k}, \alpha, \beta, \gamma)|^2. \quad (9)$$

Here,  $N_e$  is the number of electrons the molecular orbital under consideration, and  $\mu_{Ie}$ ,  $\mu_{PT}$  are the reduced electron–target and projectile–target masses:

$$\mu_{Ie} = \frac{M_I}{M_I + 1} \quad (10)$$

$$\mu_{PT} = \frac{M_P(M_I + 1)}{M_P + M_I + 1}. \quad (11)$$

If we work in terms of the rotational sudden approximation, we expect the molecular orientation in space to remain constant during the time the collision takes place. Furthermore, the molecular Euler angles are randomly distributed. Then, in order to obtain the FDCS we must average equation (9) over the Euler angles  $(\alpha, \beta, \gamma)$ :

$$\frac{d^5\sigma}{d^2\mathbf{q}_\perp d^3\mathbf{k}} = \frac{1}{8\pi^2} \int_0^\pi \sin\beta d\beta \int_0^{2\pi} d\alpha \int_0^{2\pi} d\gamma \times \frac{d^8\sigma}{d^2\mathbf{q}_\perp d^3\mathbf{k} d\alpha d\beta d\gamma}. \quad (12)$$

We refer the reader to our previous article [43] for more specific details on the calculation procedure of the FDCS including the averaging procedure over the molecular orientation and the way in which the partial wave analysis is handled.

### 3. Results

We have calculated fully differential single ionization cross sections for collisions of H<sup>+</sup>,  $\bar{p}^-$ , and He<sup>2+</sup> on H<sub>2</sub>O initially in its electronic and vibrational ground state. We have also calculated the doubly differential cross sections for the collision with He<sup>2+</sup> making a numerical integration of the projectile deflection variables  $\varphi_p$  and  $q$ . For that goal we repeated the calculation of the FDCS in a grid of about twenty-three (depending on which orbital) values for the transferred momentum from  $q = K_i - K_f$  to  $q = 2.0$  and fifteen values for the azimuthal deflection angle between  $\varphi_p = 0$  and  $\varphi_p = \pi$ , the FDCS for the third and fourth quadrant of  $\varphi_p$  were calculated by taking into account the symmetry of the collision. The calculations have been done at an impact energy of 2 MeV/amu, and for the FDCS we have considered electron emission energies of 5 and 10 eV and transferred momentum values of 0.25, 0.5 and 0.75 a.u.. In all cases

$l, m$	0, 0			1, 0		
$a, n, \xi$	0.01889	1	12.600	0.02484	2	3.920
	-0.25592	1	7.450	-0.00835	2	2.440
	0.09939	2	3.240	0.18636	2	1.510
	0.77745	2	2.200			
	0.16359	2	1.280			
$l, m$	2, 0			3, 0		
$a, n, \xi$	0.00215	3	2.400	-0.02628	4	1.950
	0.00695	3	1.600			
$l, m$	2, 2			2, -2		
$a, n, \xi$	-0.00699	3	2.400	-0.00699	3	2.400
	-0.04528	3	1.600	-0.04528	3	1.600
$l, m$	3, 2			3, -2		
$a, n, \xi$	-0.03988	4	1.950	-0.03988	4	1.950

**Table 1.** Coefficients of the expansion of the wave function of the orbital  $2A_1$  of H<sub>2</sub>O.  $E = -1.3261$  a.u.

$l, m$	0, 0			1, 0		
$a, n, \xi$	-0.00848	1	12.600	0.24413	2	3.920
	0.08241	1	7.450	0.00483	2	2.440
	-0.04132	2	3.240	0.79979	2	1.510
	-0.30752	2	2.200			
	0.14954	2	1.280			
$l, m$	2, 0			3, 0		
$a, n, \xi$	0.00396	3	2.400	-0.01929	4	1.950
	0.05935	3	1.600			
$l, m$	2, 2			2, -2		
$a, n, \xi$	0.01206	3	2.400	0.01206	3	2.400
	-0.06571	3	1.600	-0.06571	3	1.600
$l, m$	3, 2			3, -2		
$a, n, \xi$	-0.04662	4	1.950	-0.04662	4	1.950

**Table 2.** Coefficients of the expansion of the wave function of the orbital  $3A_1$  of H<sub>2</sub>O.  $E = -0.5561$  a.u.

(shown in Figures 1–6) the analysis has been restricted to the coplanar geometry in which the momenta of all the particles in the final channel live in the plane defined by  $\mathbf{K}_i$  and  $\mathbf{K}_f$ . The angle  $\theta_e$  is the emission angle of the electron in the collision plane measured clockwise from the beam direction. The projectiles are deflected counter clockwise.

In Fig. 1 we show the FDCS for single ionization of H<sub>2</sub>O by H<sup>+</sup> and  $\bar{p}^-$  impact. The emitted electron energy is 5 eV and the momentum transferred by the projectile is

$l, m$	1, 1			1, -1		
$a, n, \xi$	0.16397 $i$	2	3.920	0.16397 $i$	2	3.920
	-0.05008 $i$	2	2.440	-0.05008 $i$	2	2.440
	0.62416 $i$	2	1.510	0.62416 $i$	2	1.510
$l, m$	2, 1			2, -1		
$a, n, \xi$	-0.01404 $i$	3	2.400	-0.01404 $i$	3	2.400
	0.17992 $i$	3	1.600	0.17992 $i$	3	1.600
$l, m$	3, 1			3, -1		
$a, n, \xi$	0.03200 $i$	4	1.950	0.03200 $i$	4	1.950
$l, m$	3, 3			3, -3		
$a, n, \xi$	-0.04512 $i$	4	1.950	-0.04512 $i$	4	1.950

**Table 3.** Coefficients of the expansion of the wave function of the orbital 1B<sub>2</sub> of H<sub>2</sub>O.  $E = -0.6814$  a.u.

$l, m$	1, 1			1, -1		
$a, n, \xi$	0.17578	2	3.920	-0.17578	2	3.920
	0.08154	2	2.440	-0.08154	2	2.440
	0.50969	2	1.510	-0.50969	2	1.510
$l, m$	2, 1			2, -1		
$a, n, \xi$	0.00285	3	2.400	-0.00285	3	2.400
	0.03870	3	1.600	-0.03870	3	1.600
$l, m$	3, 1			3, -1		
$a, n, \xi$	0.00661	4	1.950	-0.00661	4	1.950
$l, m$	3, 3			3, -3		
$a, n, \xi$	-0.01903	4	1.950	0.01903	4	1.950

**Table 4.** Coefficients of the expansion of the wave function of the orbital 1B<sub>1</sub> of H<sub>2</sub>O.  $E = -0.4954$  a.u.

$q = 0.25$ . It can be seen that for the lesser bound molecular orbitals, the typical two-lobe structure appearing in single ionization of hydrogen and helium by ion and electron impact turns evident. Furthermore, we notice that for these emission geometries, the binary peak is more intense for proton impact while the recoil peak is more intense for  $\bar{p}^-$  impact. This can be expected based on the simple postcollisional influence of the receding projectile.

For the 2A<sub>1</sub> orbital, the binary to recoil peak ratio is also larger for proton impact. However, we note that the angular distributions are not as spread as those previously described. Furthermore, the FDCS for proton impact seems to be more intense than that of  $\bar{p}^-$  impact over the whole angular range. To understand these features, in Fig. 2 we present the electronic radial and momentum distributions (angularly integrated) for the different orbitals under consideration. It can be seen that the radial distribution for the 2A<sub>1</sub> orbital clearly shows the footprints of the dominant 2s component which

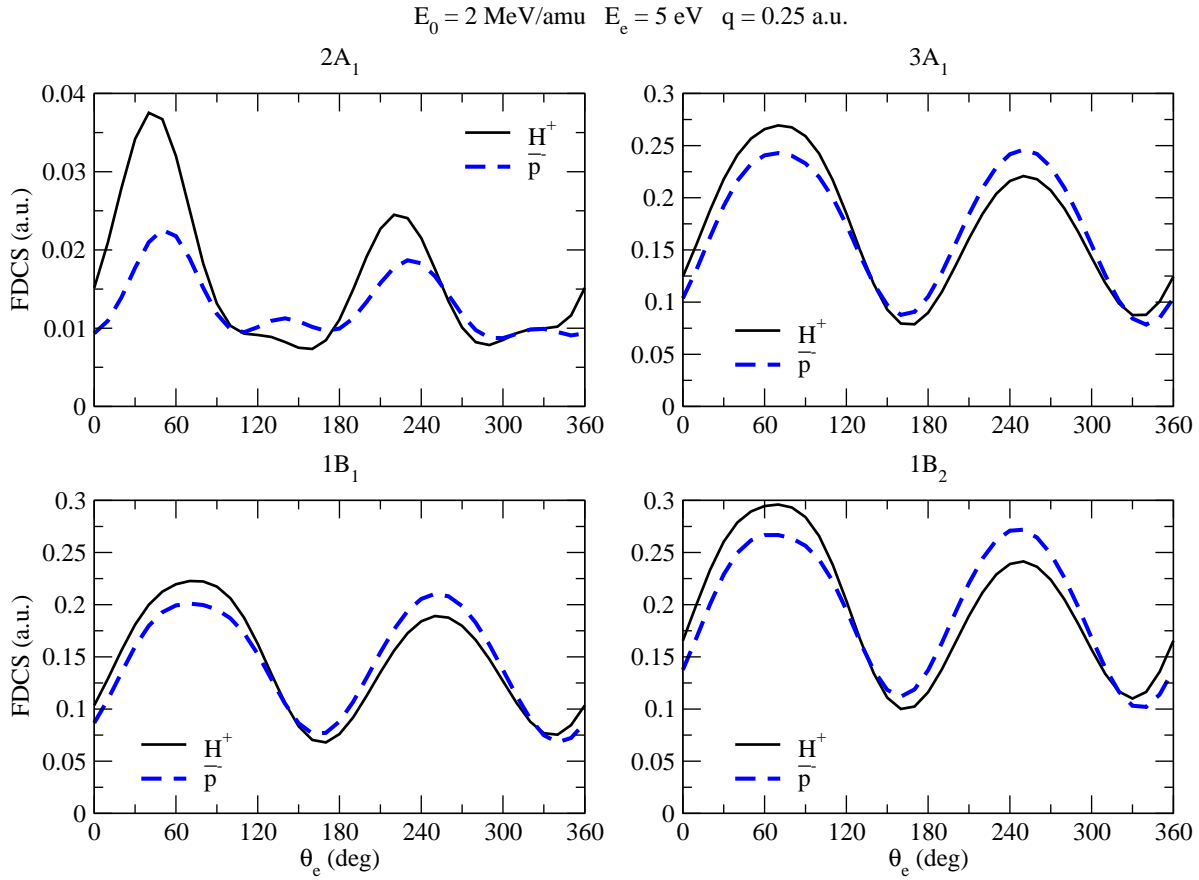


**Figure 1.** (Color online) Fully differential cross section  $\frac{d^5\sigma}{d^2q_\perp d^3k_e}$  for the single ionization of H<sub>2</sub>O by H<sup>+</sup> (full line) and  $\bar{p}$  (dashed line) impact versus the in-plane electron emission  $\theta_e$  for an impact energy of  $E_0 = 2 \text{ MeV/amu}$ , an electron emission energy of  $E_e = 5 \text{ eV}$ , and a transferred momentum  $q = 0.25 \text{ a.u.}$  The four relevant orbitals of the molecule are shown individually.

leads to a nodal structure at about  $0.25 \text{ a.u.}$  and a more compressed distribution than those corresponding to the other orbitals. However, it is in the momentum distribution where the most noticeable difference is found. The  $2A_1$  orbital presents a more localized distribution, which leads to narrower structures in the FDCS. Besides, the projectile needs to transfer a larger amount of momentum to ionize an electron from this inner orbital. It is then expected that the ionization channel for this orbital will be fed from low angular momenta (which classically would correspond to inner impact parameters) compared to the lesser bound orbitals. This physical picture leads to the expectation of a greater ionization probability for proton impact compared to the antiproton impact case in which the electron is pushed against the parent molecular ion by the receding projectile.

Similar situations are illustrated in Figs. 3 and 4 for  $q = 0.5$  and  $0.75 \text{ a.u.}$  respectively. Interestingly, for these collision geometries, the lesser bound molecular orbitals clearly exhibit a drastic change in their angular patterns. The binaries as well



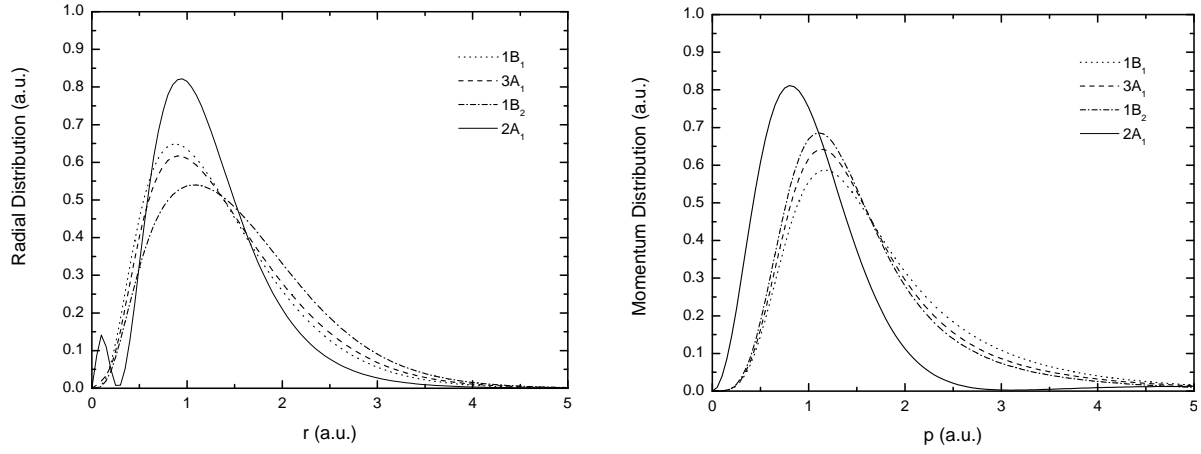


**Figure 2.** Angularly integrated Electronic Radial and Momentum distributions for the molecular orbitals under consideration

as recoil peaks are two-peak structures that can be associated to the  $p$ -nature of some of the Slaters which conform each molecular orbital. In the present case, for low  $q$  values the angular distributions lead to the typical two-peak (binary and recoil) structure as obtained for H and He targets. On the other hand, as the momentum transfer increases, the  $p$ -nature of the initial state leads to a clear splitting on each peak as can be inferred from Figs. 3 and 4, getting a two peak-structure associated to either the binary or recoil structures. Such a behavior is in agreement with recent calculations and experiments related to the single ionization of Ar(3p) by positrons and electrons [46, 47], where a similar dependence of the binary peak profile with the transferred momentum  $q$  has been inferred. As in Fig. 1, we note that for the more tightly bound orbital under consideration, the proton impact FDCS leads to more intense results compared to the antiproton impact case.

In Figs. 5 and 6 we show the single ionization FDCS for 2 MeV/amu He<sup>2+</sup> impact and an electron emission energy of 5 eV and 10 eV respectively. The FDCS corresponding to the different orbitals under consideration are shown for three different projectile momentum transfers. Trends observed are similar to those described for proton impact in Figs. 1, 3 and 4: the binary peak splits in two for increasing projectile momentum transfers. The inner orbital provides more localized structures compared to the lesser bound orbitals which spread over a larger angular range.

We now turn our attention to the doubly differential cross sections which are given by:

$$\begin{aligned} \frac{d^3\sigma}{dE_e d\Omega_e} &= \frac{1}{2K_i^2} \int_0^{2\pi} d\varphi_p \int_{K_i-K_f}^{K_i+K_f} dq \\ &\times q (K_i^2 + K_f^2 - q^2) k_e \frac{d^5\sigma}{d^2\mathbf{q}_\perp d^3\mathbf{k}}. \end{aligned} \quad (13)$$

In Figures 7 and 8, we show the DDCS for the same collision system for an impact energy of 2 and 6 MeV/amu respectively. Electron emission energies of  $E_e = 5$  and 10 eV are

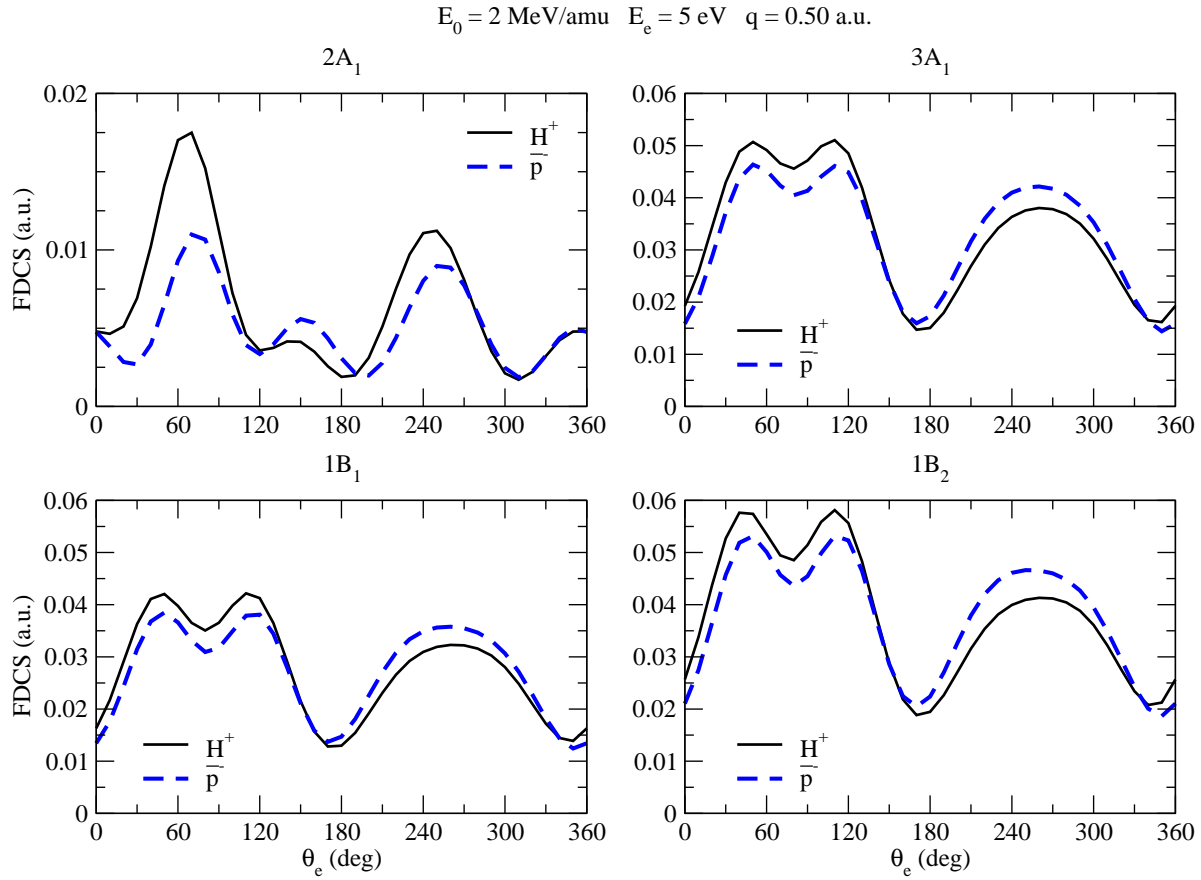


**Figure 3.** (Color online) Fully differential cross section  $\frac{d^5\sigma}{d^2q_\perp d^3k_e}$  for the single ionization of H<sub>2</sub>O by H<sup>+</sup> (full line) and  $\bar{p}^-$  (dashed line) impact at an energy of  $E_0 = 2 \text{ MeV/amu}$ , an electron emission energy of  $E_e = 5 \text{ eV}$ , and a transferred momentum  $q = 0.50 \text{ a.u.}$  The four relevant orbitals of the molecule are shown individually.

explicitly considered for the case of  $E_0 = 2 \text{ MeV/amu}$ , while for  $E_0 = 6 \text{ MeV/amu}$  we only considered the electron emission energy  $E_e = 10 \text{ eV}$ . In all cases, the DDCS are shown as a function of the electron ejection angle counted clockwise. For the lesser bound orbitals, we observe that the distributions are nearly isotropic with a maximum around  $60^\circ$ .

So far, we have been mainly concerned in the analysis of the profiles exhibited by the FDSC and DDCS for the different orbitals in terms of the electron emission angle. However, to compare to experiments another issue should be considered. Orbitals with similar ionization potentials might individually contribute to the ionization channel for a given scattering angle or, in impact parameter methods, for a given impact parameter. In this sense, the single ionization probability from one explicit orbital should take into account that no other electron is simultaneously removed from any other competing orbital. In impact parameter methods, the contribution from a given orbital to the ionization channel is then given by the probability to ionize one electron from that

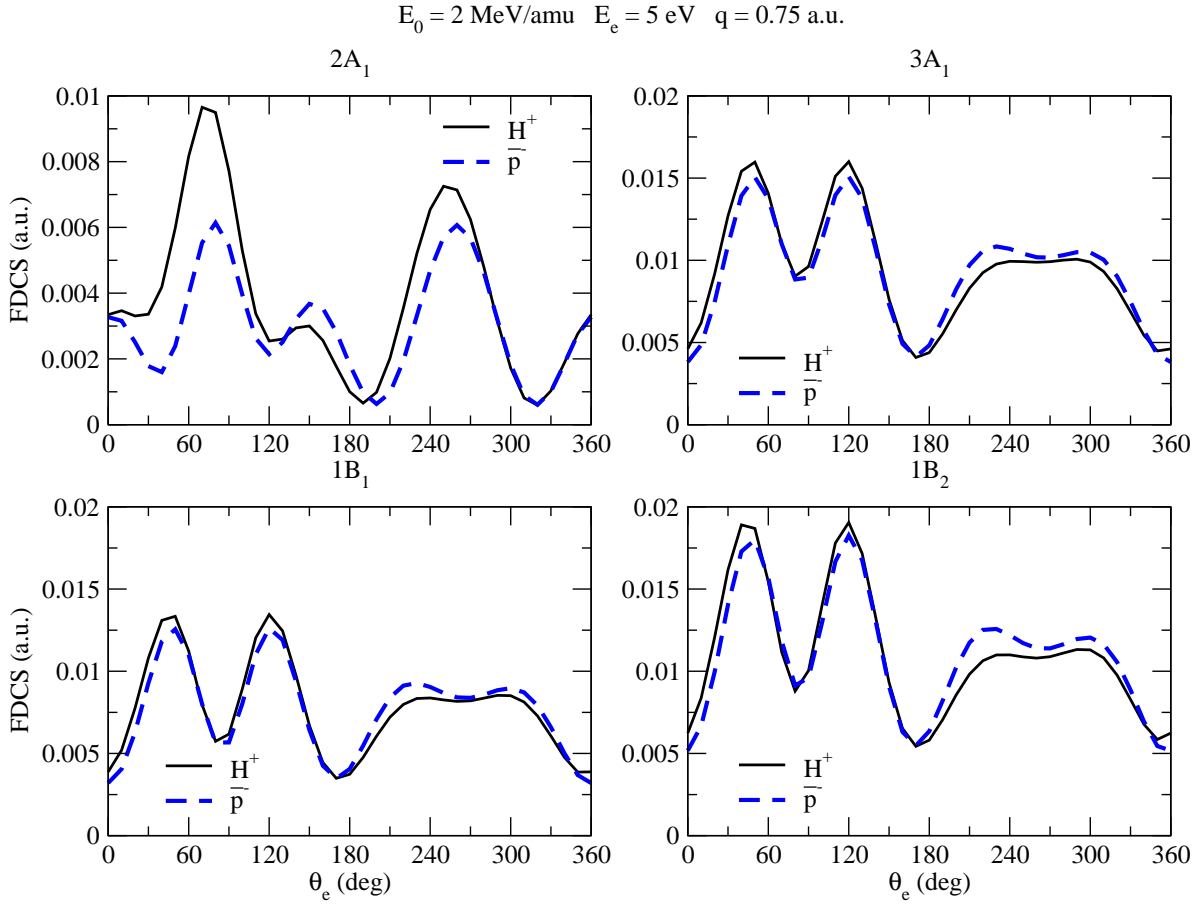


**Figure 4.** (Color online) Fully differential cross section  $\frac{d^5\sigma}{d^2q_\perp d^3k_e}$  for the single ionization of H<sub>2</sub>O by H<sup>+</sup> (full line) and  $\bar{p}^-$  (dashed line) at an energy of  $E_0 = 2 \text{ MeV/amu}$ , an electron emission energy of  $E_e = 5 \text{ eV}$ , and a transferred momentum  $q = 0.75 \text{ a.u.}$  The four relevant orbitals of the molecule are shown individually.

orbital, times the probability of no-electron removal from the remaining orbitals (see for example [36]).

Alternatively, in the present context we follow the proton impact ionization studies on H<sub>2</sub>O molecules by Luna *et al* [19] together with their reported dissociation probabilities [48] and we consider branching ratios of 0.32 for the 1B<sub>1</sub> and 3A<sub>1</sub> orbitals and 0.36 for the 1B<sub>2</sub> orbital. We note that a similar strategy has been used in recent years to address single electron capture processes on H<sub>2</sub>O molecules by bare ions at low impact energies [49]. The resulting DDCS is shown in figure 9 and is in very good agreement with the data from Ohsawa *et al* [17], which predict a practically isotropic behavior as a function of the emission angle. In the figure, we also add the calculated DDCS at 2 MeV/amu and incorporate the low energy data of Toburen to help visualize how the DDCS magnitudes decrease as the impact energy increases [50].

In figure 10 we show the integrand of the DDCS (13) after performing the first integral in the azimuthal angle of the projectile. Three electron emission angles are

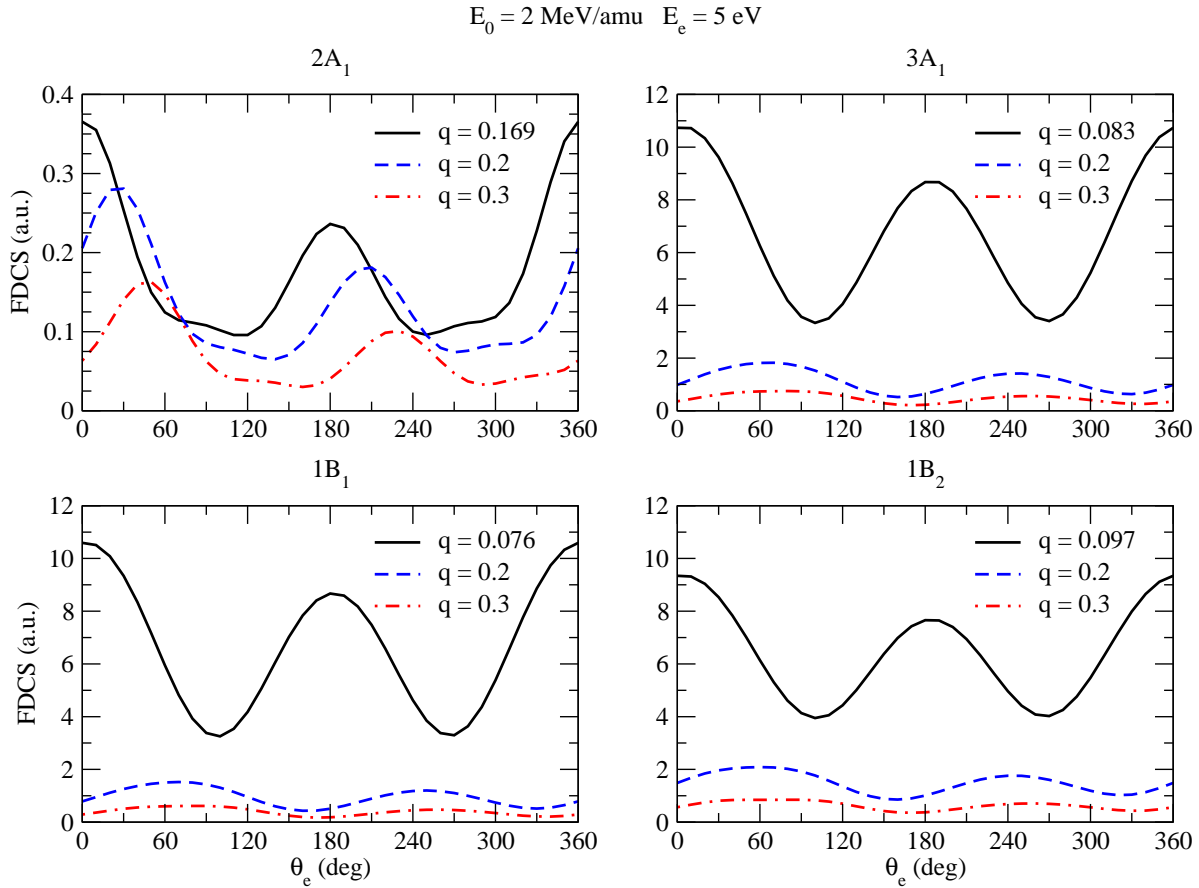


**Figure 5.** (Color online) Fully differential cross section  $\frac{d^5\sigma}{d^2q_\perp d^3k_e}$  for the single ionization of H<sub>2</sub>O by He<sup>2+</sup> impact at an energy of  $E_0 = 2 \text{ MeV/amu}$ , an electron emission energy of  $E_e = 5 \text{ eV}$ , and three values of the transferred momentum  $q = K_i - K_f$ , 0.2, 0.3 a.u. The four relevant orbitals of the molecule are shown individually.

explicitly shown. The integral is converged for a value of the transferred momentum of  $q = 2 \text{ a.u.}$  while the initial momentum values  $K_i = 53747 \text{ a.u.}$

Once the molecular orientation and the projectile deflection angles are averaged, the system gains the cylindrical symmetry. As a result, the DDCS shown in Fig. 7 is symmetrical with respect to the 180° angle. We can calculate then the Single Differential Cross Section (SDCS) with a single integral using this symmetry as

$$\frac{d\sigma}{dE_e} = 2\pi \int_0^\pi \sin\theta_e d\theta_e \frac{d^3\sigma}{dE_e d\Omega_e}. \quad (14)$$

In table 5 we show the calculated SDCS for the two energies for the ejected electron calculated in present work. After using the above mentioned branching ratios, the estimated SDCS read at 2 MeV/amu,  $7.47 \times 10^{-18} \text{ cm}^2/\text{eV}$  (5 eV) and  $4.11 \times 10^{-18} \text{ cm}^2/\text{eV}$  (10 eV). On the other hand, at 6 MeV/amu impact energy and 10 eV emission energy, the estimated SDCS reads  $1.72 \times 10^{-18} \text{ cm}^2/\text{eV}$ .

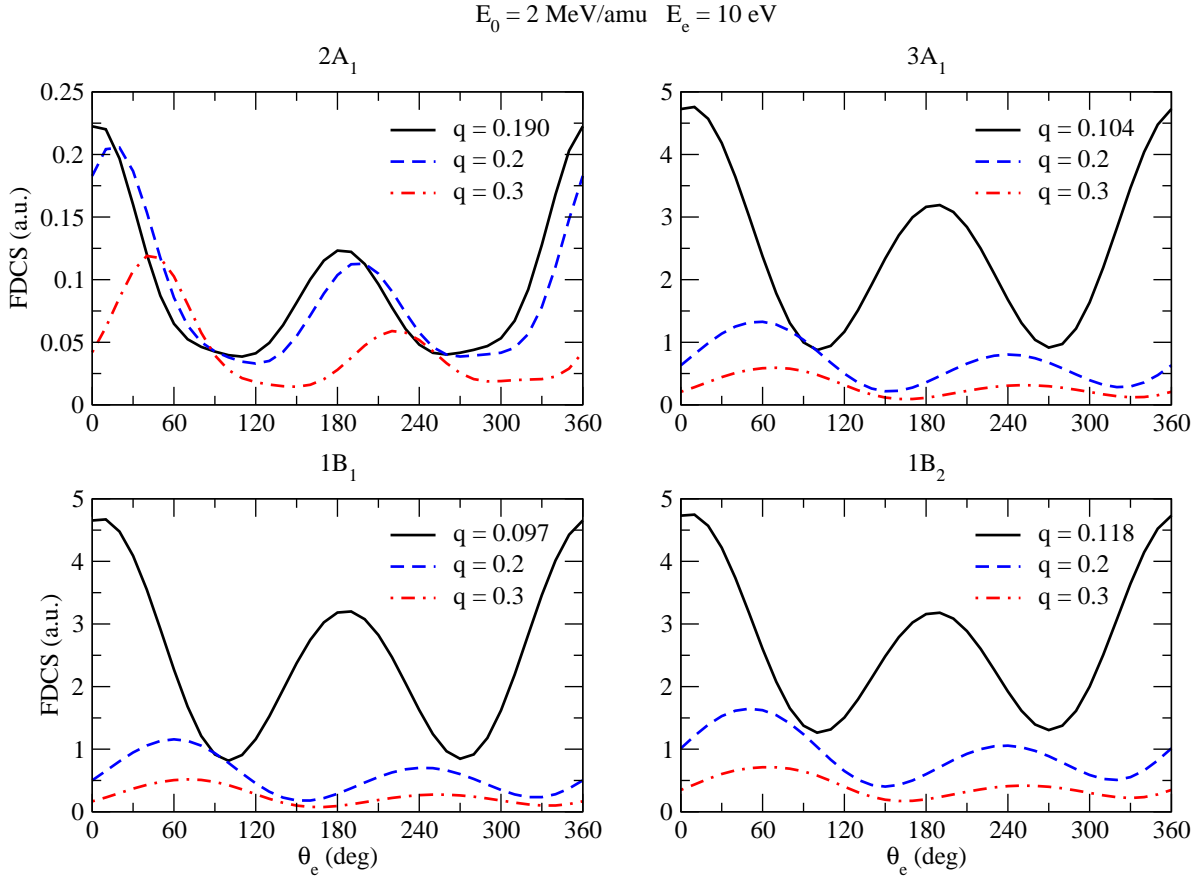


**Figure 6.** (Color online) Fully differential cross section  $\frac{d^5\sigma}{d^2q_\perp d^3k_e}$  for the single ionization of H<sub>2</sub>O by He<sup>2+</sup> impact at an energy of  $E_0 = 2 \text{ MeV/amu}$ , an electron emission energy of  $E_e = 10 \text{ eV}$ , and three values of the transferred momentum  $q = K_i - K_f$ , 0.2, 0.3 a.u. The four relevant orbitals of the molecule are shown individually.

$E_0 = 2 \text{ MeV/amu}$				
$E_e$ (eV)	$2A_1$	$3A_1$	$1B_1$	$1B_2$
5	1.0858	6.7408	5.7367	9.0845
10	0.6406	3.6306	3.1628	5.0725
$E_0 = 6 \text{ MeV/amu}$				
10	0.236592	1.52881	1.30747	2.13355

**Table 5.** Electron ejection angles integrated single differential cross section  $\frac{d\sigma}{dE_e}$  (a.u.) for the single ionization of H<sub>2</sub>O by He<sup>2+</sup> impact at an energy of  $E_0 = 2$  and 6 MeV/amu, and electron emission energies of  $E_e = 5$  and 10 eV. The four relevant orbitals of the molecule are shown individually.

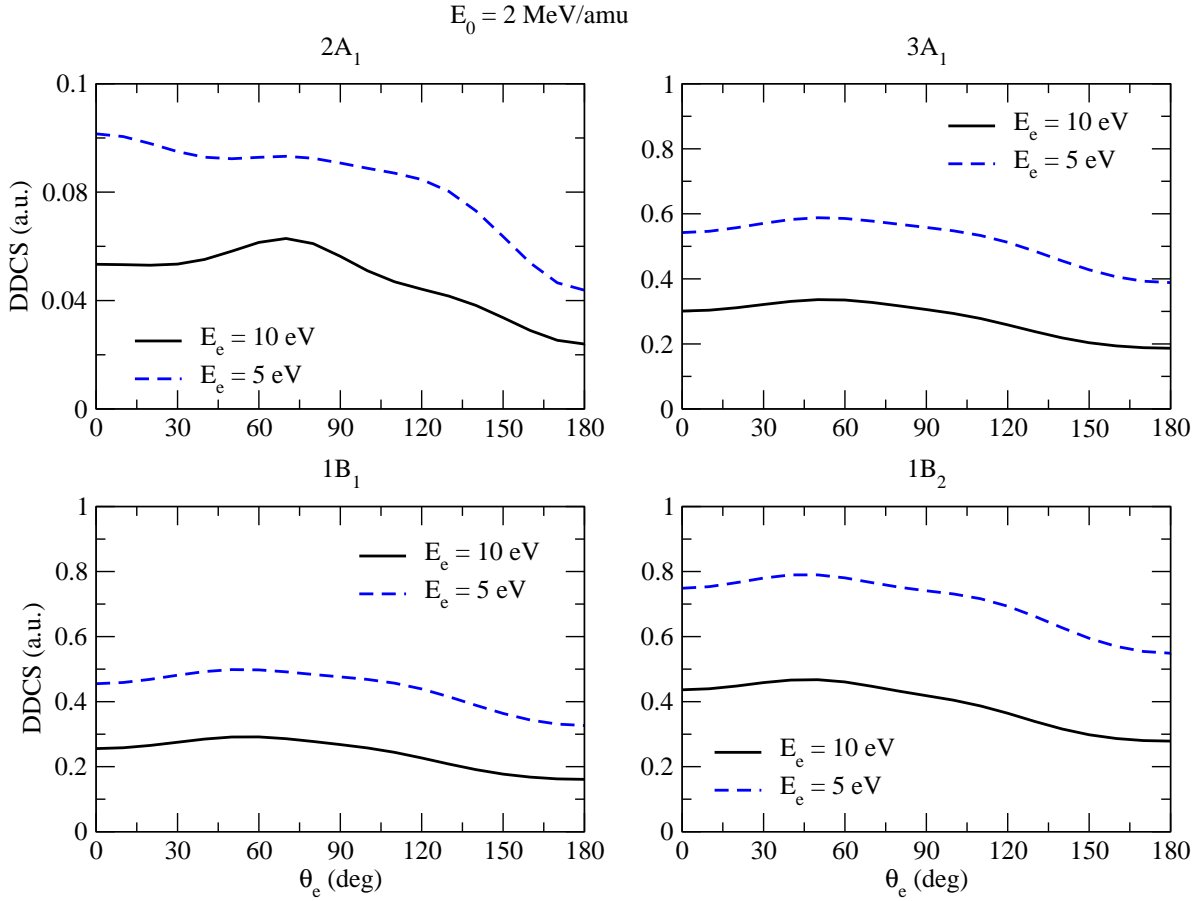


**Figure 7.** (Color online) Projectile angle integrated double differential cross section  $\frac{d^3\sigma}{dE_e d\Omega_e}$  for the single ionization of H<sub>2</sub>O by He<sup>2+</sup> impact at an energy of  $E_0 = 2$  MeV/amu, an electron emission energy of  $E_e = 5$  and 10 eV. The four relevant orbitals of the molecule are shown individually.

#### 4. Conclusions

In this work we have studied the single ionization of the water molecule at the fully and doubly differential level. The present study has been performed by using a recently developed distorted wave model which considers a model central potential for the emitted electron-molecular ion interaction.

The present results suggest that for low momentum transfers and low energy emitted electrons, the typical two-lobe (binary-recoil) profile is obtained. As the momentum transfer increases, these structures evolve into more complex ones, splitting due to the  $p$ -character of the molecular orbitals under study. These results are in agreement with recent experimental and theoretical studies on FDCS for the single ionization of Ar(3p) by electrons and positrons [46, 47].

For the inner orbital under consideration ( $2A_1$ ), we noticed that the calculated FDCS present narrower structures compared to those obtained for the lesser bound molecular orbitals. We ascribe this feature to the more localized electronic momentum

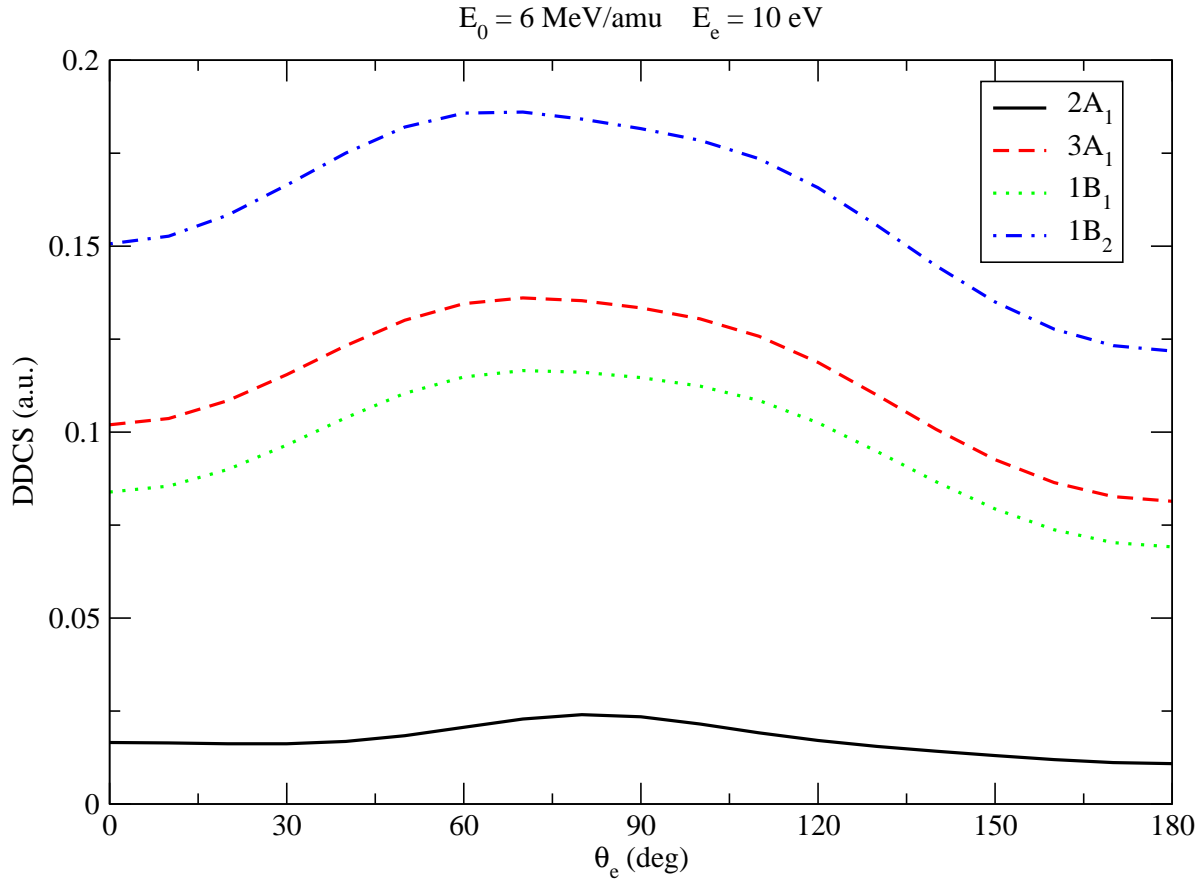


**Figure 8.** (Color online) Projectile angle integrated double differential cross section  $\frac{d^3\sigma}{dE_e d\Omega_e}$  for the single ionization of H<sub>2</sub>O by He<sup>2+</sup> impact at an energy of  $E_0 = 6 \text{ MeV/amu}$ , an electron emission energy of 10 eV. The four relevant orbitals of the molecule are shown individually.

distribution.

We have also calculated the DDCS for the collision of He<sup>2+</sup> with H<sub>2</sub>O, from the different molecular orbitals finding very good agreement with the experimental data of Ohsawa *et al* at an impact energy of 6 MeV/amu. To achieve convergence in the integration procedures, we needed a grid of twenty three values of the transferred momentum  $q$ , depending on the orbital, and fifteen values of the azimuthal deflection angle of the projectile  $\varphi_p$  for each point of the graphic 7. That took two months of calculation for each electron energy occupying four hundred nodes on the computation cluster at IPP-Garching. This proves that the present model, conceived to improve the description at the fully differential level, is ineffective to obtain integrated values, and absolutely not usable to get the total cross sections. Other methods, like CTMC, proved through the years to be effective and fast to provide integrated cross sections while computation time drastically increases as we move to fully differential data. In this sense, complementary strategies should be conceived to identify and fill the gaps in ionization cross sections databases that could be relevant in different fields.

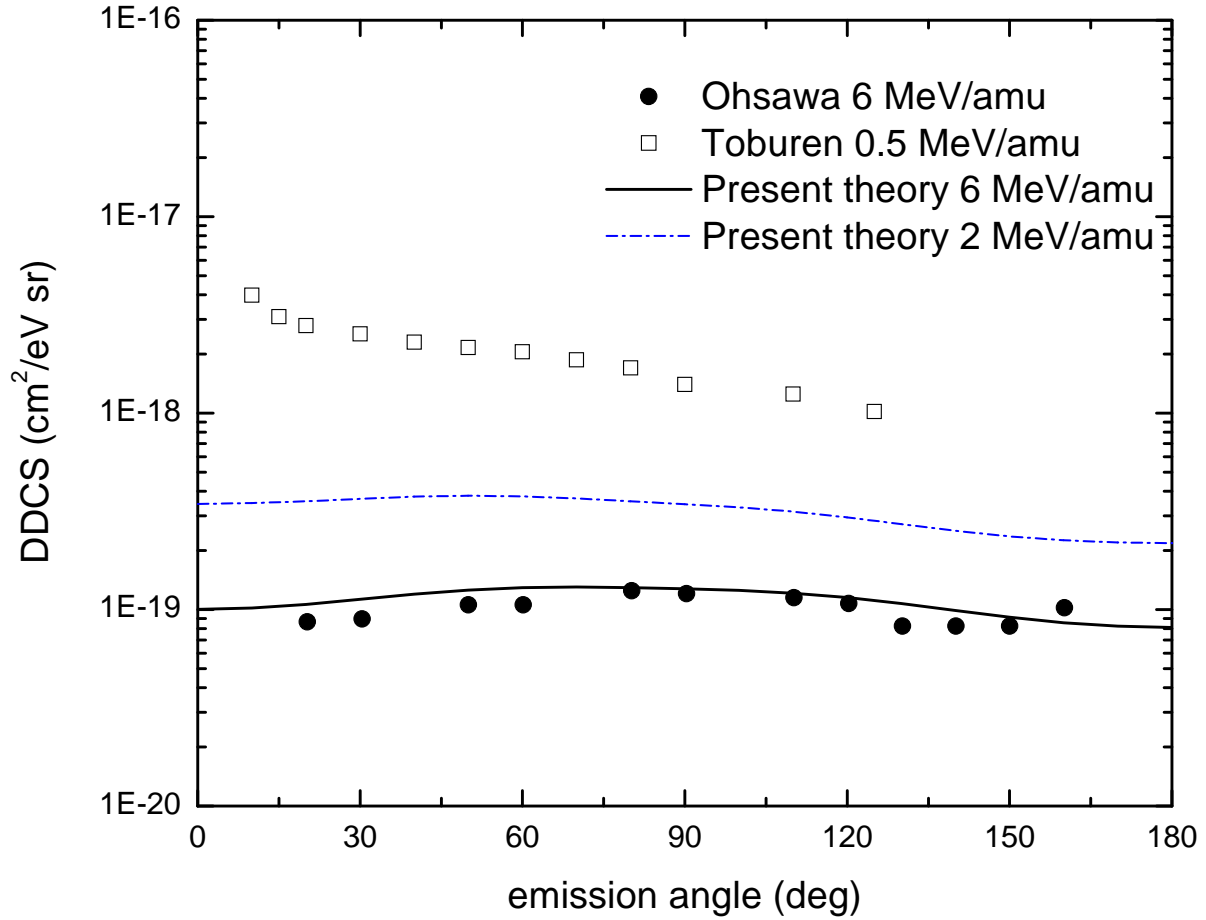


**Figure 9.** Calculated DDCS as a function of electron emission angle at impact energy 2 and 6 MeV/amu and electron emission energy of 10 eV. —: present work; • 6 MeV/amu data of Ohsawa *et al* [17]; □ 0.5 MeV/amu data of Toburen [50].

We have concentrated on collision and emission energies that are accessible with the COLTRIMS technique (low  $q$  values, low-energy electron emission) although water is not an easy target to deal with COLTRIMS. Experiments recently performed with such reaction microscope employing water target in vapor phase at a target temperature of 383 K involved the measurement of the kinetic energy release of the ionic fragments [51]. We note, on the other hand, that FDCS for the single ionization of water molecules by electrons have been measured in recent years using an electron coincidence spectrometer [52]. In this sense, we hope that experimental data for the single ionization of water by ion impact will be available in the next few years. That would help us to further test and refine the theoretical models currently under use and provide reliable data that could fill the gaps in cross sections databases for medical and astrophysical applications.



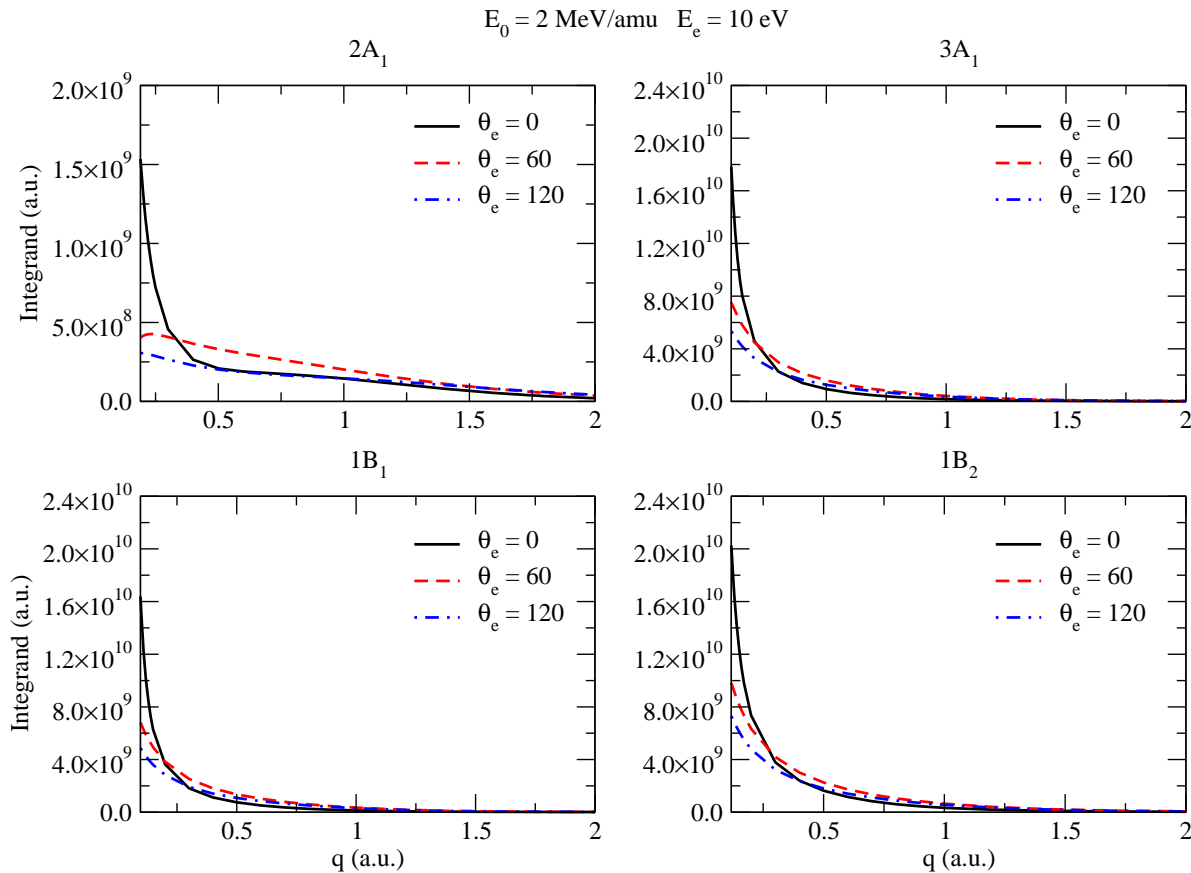


**Figure 10.** (Color online) Integrand of equation (13) for the single ionization of H<sub>2</sub>O by He<sup>2+</sup> impact at an energy of  $E_0 = 2 \text{ MeV/amu}$ , an electron emission energy of  $E_e = 10 \text{ eV}$ , and three values of the electron in plane ejection angle of  $\theta_e = 0, 60^\circ, 120^\circ$ . The four relevant orbitals of the molecule are shown individually.

## Acknowledgments

This work has been supported by Universidad Nacional del Sur (Project No. PGI 24/F059), and Consejo Nacional de Investigaciones Científicas y Técnicas, Argentina (Project No. PIP 112-201101-00749). The calculations were carried out in the TOK-Linux cluster in the Max Planck Institut für Plasmaphysik in Garching and computing clusters of APAP project in University of Strathclyde. We thank Prof. L. Toburen for sending us his data in tabular form.

- [1] Stolterfoht N, Dubois RD, Rivarola RD. *Electron Emission in Heavy Ion-Atom Collisions*. Springer, New York; 1997.
- [2] Rescigno TN, Baertschy M, Isaacs WA, McCurdy CW. *Science*. 199;286:2474.
- [3] Baertschy M, Rescigno TN, McCurdy CW. *Phys Rev A*. 2001;64:022709.
- [4] Bray I, Fursa DV, Kadyrov AS, Stelbovics AT. *Phys Rev A*. 2010;81:062704.
- [5] Amaldi U, Kraft G. *Rep Prog Phys*. 2005;68:1861.
- [6] Ulrich J, Moshhammer R, Dörner R, Jagutzki O, Mergel V, Schmidt-Böking H, et al. *J Phys B: At Mol Opt Phys*. 1997;30:2917.
- [7] Dörner R, Mergel V, Ali R, Buck U, Cocke CL, Froschauer K, et al. *Phys Rev Lett*. 1994;72:3166–

3169.

- [8] Moshhammer R, Ullrich J, Unverzagt M, Schmitt W, Schmidt-Böcking B. *Nuclear Instruments and Methods in Physics Research B: Beam Interactions with Materials and Atoms.* 1996;108:425 – 445.
- [9] Dörner R, Bräuning H, Feagin JM, Mergel V, Jagutzki O, Spielberger L, et al. *Phys Rev A.* 1998;57:1074–1090.
- [10] Dörner R, Mergel V, Spielberger L, Jagutzki O, Ullrich J, Schmidt-Böcking H. *Phys Rev A.* 1998;57:312–317.
- [11] Mergel V, Dörner R, Khayyat K, Achler M, Weber T, Jagutzki O, et al. *Phys Rev Lett.* 2001;86:2257–2260.
- [12] Dörn A, Kheifets A, Schröter CD, Najjari B, Höhr C, Moshhammer R, et al. *Phys Rev Lett.* 2001;86:3755–3758.
- [13] Nguyen H, Brédy R, Camp HA, Awata T, DePaola BD. *Phys Rev A.* 2004;70:032704.
- [14] Schmidt LPH, Schöffler MS, Stiebing KE, Schmidt-Böcking H, Dörner R, Afaneh F, et al. *Phys Rev A.* 2007;76:012703.
- [15] Guan X, Bartschat K. *Phys Rev Lett.* 2009;103:213201.
- [16] Alessi M, Otranto S, Focke P. *Phys Rev A.* 2011 Jan;83:014701.
- [17] Ohsawa D, Sato Y, Okada Y, Shevelko VP, Soga F. *Phys Rev A.* 2005;72:062710.
- [18] García PMY, Sigaud GM, Luna H, Santos ACF, Montenegro EC, Shah MB. *Phys Rev A.* 2008;77:052708.
- [19] Luna H, de Barros ALF, Wyer JA, Scully SWJ, Lecointre J, García PMY, et al. *Phys Rev A.* 2007;75:042711.
- [20] Martin S, Brédy R, Allouche AR, Bernard J, Salmoun A, Li B, et al. *Phys Rev A.* 2008;77:062513.
- [21] Alessi M, Cariatore ND, Focke P, Otranto S. *Phys Rev A.* 2012 Apr;85:042704.
- [22] Hoener M, Bostedt C, Schorb S, Thomas H, Foucar L, Jagutzki O, et al. *Phys Rev A.* 2008;78:021201.
- [23] Champion C, Dal Cappello C, Houamer S, Mansouri A. *Phys Rev A.* 2006;73:012717.
- [24] Champion C, Boudrioua O, Dal Cappello C, Sato Y, Ohsawa D. *Phys Rev A.* 2007;75:032724.
- [25] Dal Cappello C, Champion C, Boudrioua O, Lekadir H, Sato Y, Ohsawa D. *Nuclear Instruments and Methods in Physics Research B: Beam Interactions with Materials and Atoms.* 2009;267:781–790.
- [26] Martínez S, Otranto S, Garibotti CR. *Phys Rev A.* 2008;77:024701.
- [27] Godunov AL, Whelan CT, Walters HRJ. *Phys Rev A.* 2008;78:012714.
- [28] Fiol J, Olson RE. *J Phys B: At Mol Opt Phys.* 2002;35:1759.
- [29] Fiol J, Otranto S, Olson RE. *J Phys B: At Mol Opt Phys.* 2006;39:L285.
- [30] Ohsawa D, Tawara H, Okada T, Soga F, Galassi ME, Rivarola RD. *J Phys: Conf Ser.* 2012;388:102029.
- [31] Champion C, Galassi ME, Weck PF, Fojón O, Hanssen J, Rivarola RD. *J Phys: Conf Ser.* 2012;388:102003.
- [32] Fiol J, Olson RE. *J Phys B: At Mol Opt Phys.* 2004;37:3947.
- [33] Otranto S, Olson RE, Fiol J. *J Phys B: At Mol Opt Phys.* 2006;39:L175–L183.
- [34] Errea LF, Illescas C, Méndez L, Pons B, Rabadán I, Riera A. *Phys Rev A.* 2007;76:040701.
- [35] Illescas C, Errea LF, Méndez L, Pons B, Rabadán I. *J Phys: Conf Ser.* 2012;388:102007.
- [36] Illescas C, Errea LF, Méndez L, Pons B, Rabadán I, Riera A. *Phys Rev A.* 2011;83:052704.
- [37] Lüdde HJ, Spranger T, Horbatsch M, Kirchner T. *Phys Rev A.* 2009;80:060702(R).
- [38] Dubois A, Carniato S, Fainstein PD, Hanssen JP. *Phys Rev A.* 2011;84:012708.
- [39] Martínez P, Errea LF, Méndez L, Rabadán I. *J Phys: Conf Ser.* 2012;388:102034.
- [40] Kirchner T, Murakami M, Horbatsch M, Lüdde HJ. *J Phys: Conf Ser.* 2012;388:012038.
- [41] Champion C, Hanssen J, Hervieux PA. *Phys Rev A.* 2001;63:052720.
- [42] Champion C, Hanssen J, Hervieux PA. *Phys Rev A.* 2005;72:059906(E).
- [43] Fernández-Menchero L, Otranto S. *Phys Rev A.* 2010;82:022712.

- [44] Tóth I, Nagy L. J Phys B: At Mol Opt Phys. 2010;43:135204.
- [45] Moccia R. J Chem Phys. 1964;40:2164.
- [46] de Lucio OG, Otranto S, Olson RE, DuBois RD. Phys Rev Lett. 2010;104:163201.
- [47] Otranto S, Olson RE. Phys Rev A. 2009;80:012714.
- [48] Montenegro EC. Journal of Physics: Conference Series. 2009;194(1):012049.
- [49] Otranto S, Olson RE. Phys Rev A. 2008 Feb;77:022709.
- [50] Toburen LH. Private communication. 2013;.
- [51] Sann H, Jahnke T, Havermeier T, Kreidi K, Stuck C, Meckel M, et al. Phys Rev Lett. 2011;106:133001.
- [52] Milne-Brownlie DS, Cavanagh SJ, Lohmann B, Champion C, Hervieux PA, Hanssen J. Phys Rev A. 2004;69:032701.